

# Some observations on the wear of single point diamond tools used for machining glass

R. E. GLARDON, I. FINNIE

*Department of Mechanical Engineering, University of California, Berkeley, CA 94720, USA*

The wear pattern on a single point diamond tool used for machining glass is studied. Possible wear mechanisms are proposed on the basis of additional sliding wear tests and observations by scanning electron and optical microscopy. The wear process is believed to take place in two stages, one involving a polishing mechanism and the other consisting of crack propagation which occurs after the accumulation of a certain amount of damage. The importance of the crystallographic orientation of the diamond single crystal, particularly for crack propagation along cleavage planes is pointed out. It is concluded that the likelihood of rapid deterioration of the diamond tool may be decreased by proper crystallographic orientation.

## 1. Introduction

Recently, attempts have been made to machine glass in a manner similar to ductile metals by using single-point diamond tools [1-3]. This work has been motivated by the successful use of single-point diamond tools in the production of metallic parts with surface finish of optical quality [4]. However, diamond has been shown to wear relatively rapidly when rubbed against glass [1, 5]. As the geometry of the contact zone between the tip of the tool and the work-piece is extremely important for the attainment of flow rather than fracture in cutting, it appears that the wear of the diamond tool may be a limiting factor in developing machining processes for glass.

The wear of diamond in general has been the subject of controversial studies and is still not well understood [6]. In particular, the mechanisms responsible for the rapid wear of diamond on glass are not known. A study of the wear of diamond tools on glass is therefore of interest, not only for that particular reason, but also for the more general problem of the wear of diamond.

In this paper, the wear pattern formed on a diamond tool used for machining glass is reported and analysed. These observations are compared

with sliding wear experiments conducted with a new diamond tool on glass plates. The results are discussed in terms of proposed wear mechanisms of diamond. Tentative conclusions are also drawn concerning the importance of tool wear in the machining of glass.

## 2. Experimental procedures

The tools investigated in this work were round nosed single crystal diamonds. Their geometry and dimensions are described in Fig. 1. The rake angle  $\alpha$  and the angles  $\gamma$  and  $\delta$  are defined on the same figure. It should be noted that these angles are measured with reference to the  $x$ -,  $y$ -, and  $z$ -axes which stay fixed in space. The diamond in the tool used for machining was mounted with built in angles  $\alpha_0 \approx -2^\circ$  and  $\delta_0 \approx 2^\circ$ . The steel base to which the diamond is attached was rotated about the  $x$ -axis to provide the two different cutting positions visible in Fig. 2. Position A corresponds to a rotation of  $\gamma = -45^\circ$  and position B to a rotation of  $\gamma = -20^\circ$ . The machining tests were run at a linear speed of  $\sim 30 \text{ mm sec}^{-1}$  using a fixed depth of penetration. Additional technical details are reported elsewhere [1]. The wear patterns were observed by standard optical microscopy

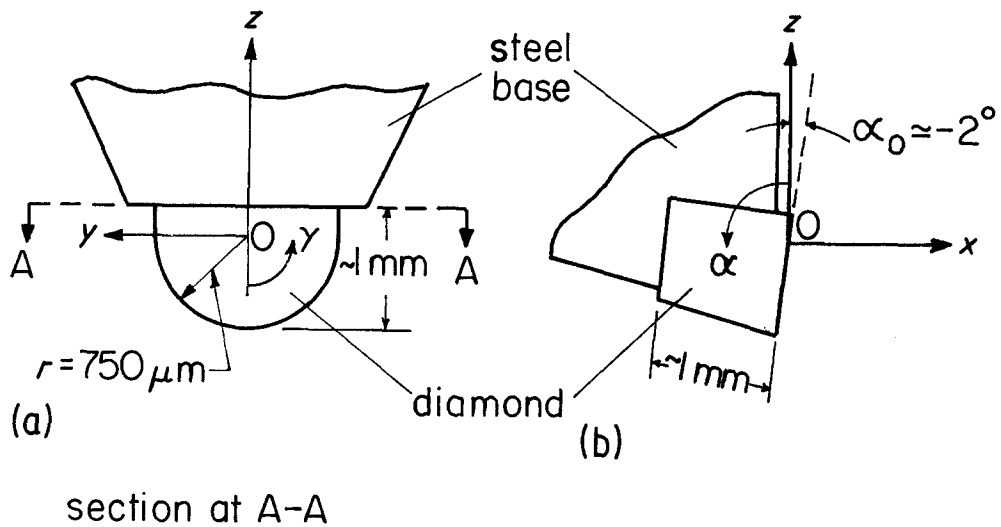


Figure 1 Geometry and dimensions of the diamond tools; (a) front view, (b) side view, (c) top view. O is the centre of the rake face. Ox is parallel to the sliding direction. Oy is perpendicular to the sliding direction and parallel to the sliding surface. Oz is perpendicular to the sliding surface. The angles  $\alpha$ ,  $\gamma$  and  $\delta$  represent the rotations around the axes Oy, Ox and Oz, respectively.

specimen rotating at a speed of 12 rpm. This corresponds to an average linear speed of  $30 \text{ mm sec}^{-1}$ . No lubricant was used and the tests were run in air at a temperature of  $\sim 23^\circ \text{C}$ . It should be noted that these conditions did not lead to a ductile machining of the glass surface, but that typical partial cone cracks were observed along the track. The tool was periodically removed for observation by SEM and optical microscopy.

and scanning electron microscopy (SEM). The crystallographic orientation of the diamond was determined by the Laue X-ray back reflection method.

In addition to the investigation of the tool used for machining experiments on glass, wear tests were conducted on a new tool. This was carried out on a modified pin on a disc wear tester which permits the measurement of the friction force. The diamond tool was loaded with a dead weight of 4 N and allowed to slide on a soda-lime glass disc

### 3. Results

#### 3.1. Tool used for machining experiments on glass

The worn areas A and B on the tool edge are shown in Fig. 2. Careful examination of these zones by optical microscopy, at magnifications up

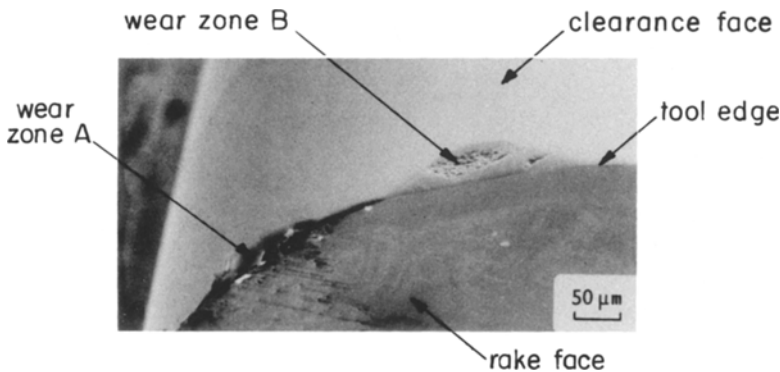


Figure 2 SEM micrograph of the edge of the tool used for machining tests on glass.

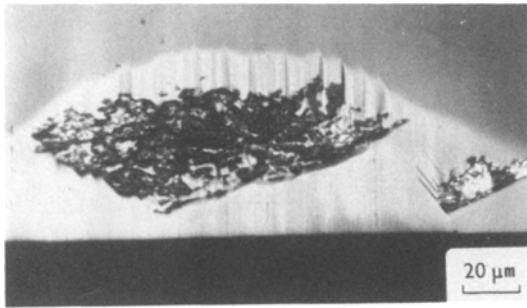


Figure 3 Optical micrograph of wear zone B.

to  $\times 1000$ , has shown that they are plane surfaces, as can be seen in Fig. 3. The orientation of these planes corresponds to that of the glass surface during machining. Thus, the wear process generates a wear plane parallel to the surface of the work-piece. As apparent in Fig. 2, areas A and B exhibit dissimilar patterns. Zone A has the appearance of a polished smooth surface, without any observable cracking. On the other hand, zone B is severely cracked on part of the surface, the rest of the wear plane having the same smooth appearance as zone A. SEM examination at high magnification ( $\times 10000$ ) and at grazing angle has revealed fine "polishing" lines running perpendicular to the tool edge on the smooth areas of the wear planes. More details of zone B can be seen on Fig. 4. As shown by Fig. 4a and b, the smooth areas of the wear plane have different appearances in front of and behind the cracked zone. Between the tool edge and the cracked zone, the surface is flat and fine "polishing" lines are visible (some of them can be seen on Fig. 4b). On the contrary, the area between the cracked zone and the clearance face consists of relatively wide grooves. This pattern is believed to be due to the abrasive effect of the diamond particles released by fracturing of the cracked zone. Fig. 4 shows also that fracture occurs mainly along two well defined directions, named  $u$  and  $v$ . These lines and that formed by the intersection of the wear plane with the rake face form the three angles  $u/v$ ,  $u/w$  and  $v/w$ , as defined in Fig. 4c. The values of these angles, measured on optical micrographs are indicated in Table I.

The determination of the crystallographic orientation of the diamond showed that the rake face is close to a  $\{001\}$  plane. It is inclined to this crystallographic direction by angles  $\alpha_r = 7^\circ$  and  $\delta_r = -3^\circ$ . Additional information concerning the orientation of the diamond is given by the stereographic projection of Fig. 5.

Fracture of diamond is known to occur by cleavage, the  $(111)$  plane being the dominant cleavage plane [7]. Therefore, the traces of the  $\{111\}$  cleavage planes on the wear planes A and B were determined. They are shown, together with the trace of the rake face, on the stereographic projections of Fig. 6. A first comparison of Figs 4 and 6b indicates the existence of an approximate correlation between the main fracture directions  $u$  and  $v$  and the traces of the  $(\bar{1}11)$  and  $(\bar{1}\bar{1}1)$  planes, respectively. To verify this observation, the angles defined by the trace of the rake face and those of planes  $(\bar{1}11)$  and  $(\bar{1}\bar{1}1)$  on wear plane B were measured on optical micrographs. Their values are reported in Table I. They correspond, within the accuracy of the method, to the angles  $u/v$ ,  $u/w$  and  $v/w$ .

### 3.2. Friction and wear tests on soda-lime glass

From the measurement of the friction force during the experiment, a value of  $\sim 0.1$  was determined for the coefficient of friction. Periodic examination of the tool after increasing sliding distances indicated the formation of wear planes parallel to the surface of the glass specimen. This is similar to the pattern observed on the worn tool used for machining experiments (Fig. 3). However, no indication of cracking was found up to a sliding distance of 200 m. The simple geometry of the wear zone allows the volume loss to be calculated. This can be done from the geometrical parameters of the tool and the dimensions of the wear plane measured by optical microscopy. The total volume loss determined in this way is represented as a function of the sliding distance in Fig. 7. While an important initial loss of material was found up to a sliding distance of 30 m, no additional measur-

TABLE I Angles between fracture directions and traces of cleavage planes on wear plane B

Fracture directions	$u/v$ $105^\circ$	$u/w$ $128^\circ$	$v/w$ $23^\circ$
Traces of cleavage planes	$\bar{1}11/\bar{1}\bar{1}1$ $107^\circ$	$\bar{1}11/\text{rake face}$ $129^\circ$	$\bar{1}\bar{1}1/\text{rake face}$ $22^\circ$

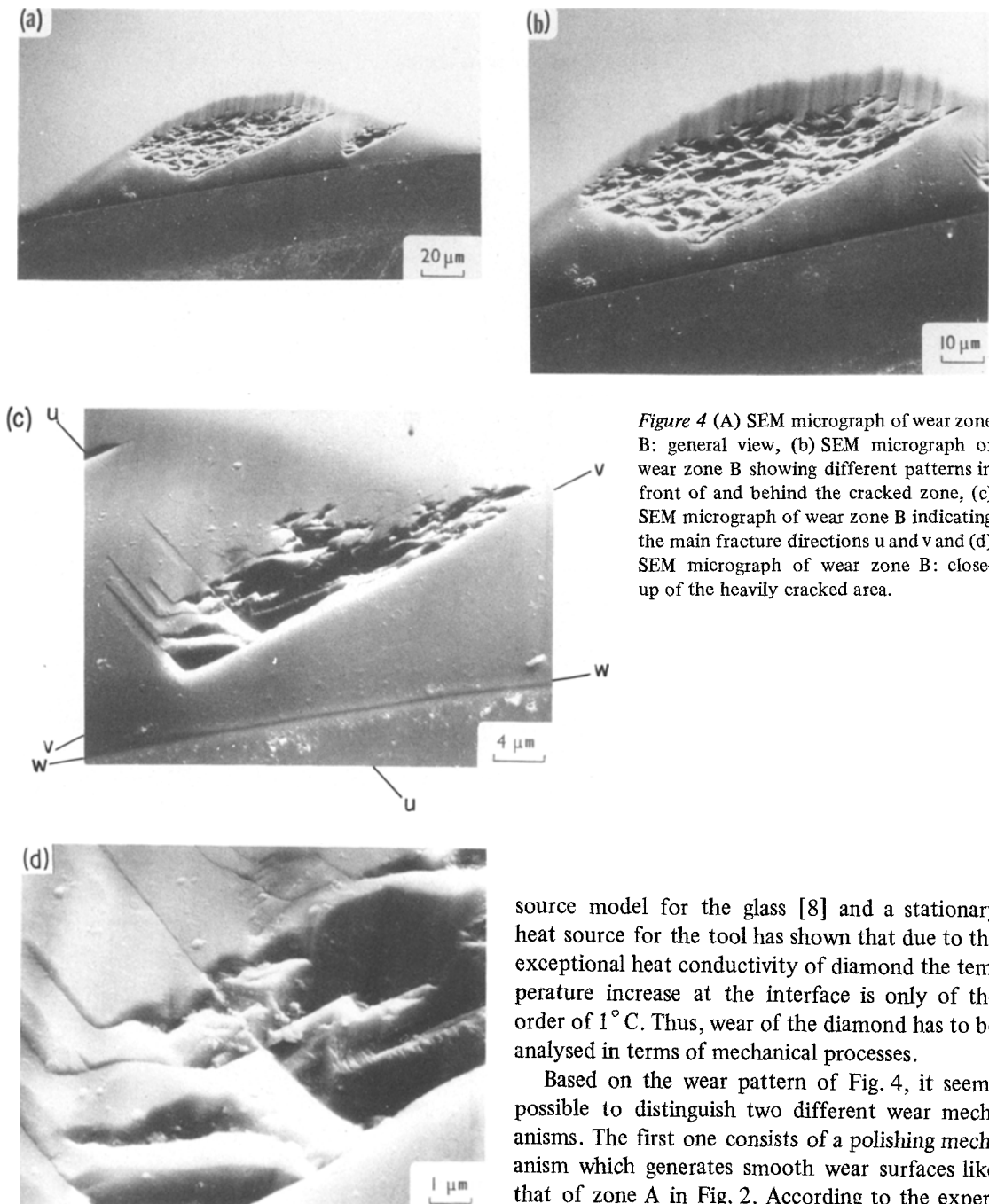


Figure 4 (A) SEM micrograph of wear zone B: general view, (b) SEM micrograph of wear zone B showing different patterns in front of and behind the cracked zone, (c) SEM micrograph of wear zone B indicating the main fracture directions u and v and (d) SEM micrograph of wear zone B: close-up of the heavily cracked area.

able wear was detected after 200 m. Although the scarcity of the experimental data limits the validity of any conclusion, it appears that, after an incubation period, the wear rate of the diamond tool remains very low.

#### 4. Discussion

An approximate calculation using a moving heat

source model for the glass [8] and a stationary heat source for the tool has shown that due to the exceptional heat conductivity of diamond the temperature increase at the interface is only of the order of  $1^{\circ}\text{C}$ . Thus, wear of the diamond has to be analysed in terms of mechanical processes.

Based on the wear pattern of Fig. 4, it seems possible to distinguish two different wear mechanisms. The first one consists of a polishing mechanism which generates smooth wear surfaces like that of zone A in Fig. 2. According to the experimental data given in Fig. 7, the corresponding wear rate should be very low. Such a polishing mechanism has been described by Wilks and Wilks [9] to be due to microcleavage on a very fine scale. The second mechanism is one involving crack propagation along cleavage planes. This process, responsible for the large scale fracturing of the wear surface shown in Fig. 4, would certainly lead to a much higher wear rate and probably to a rapid deterioration of the tool. It is interesting to note

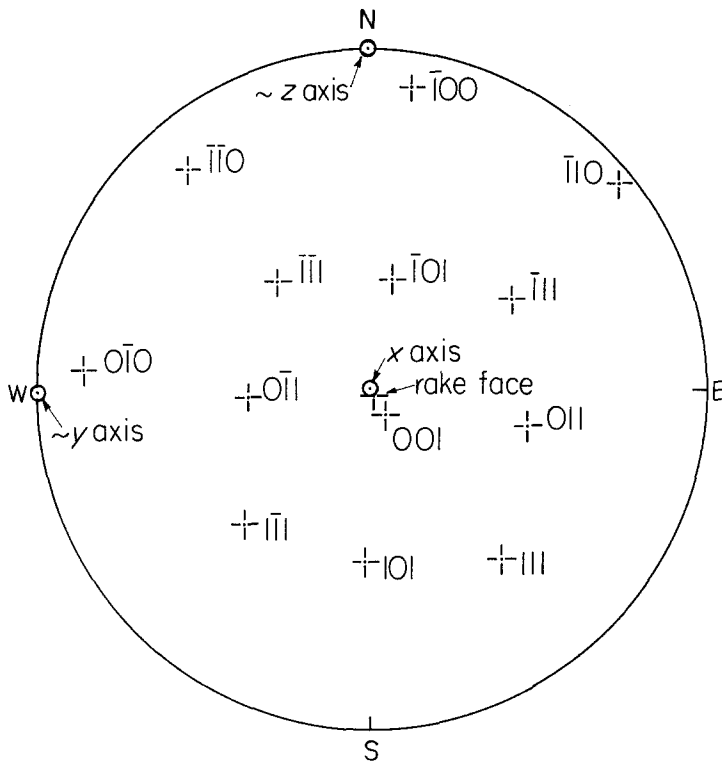


Figure 5 Stereographic projection indicating the crystallographic orientation of the diamond tool used for machining tests on glass. The plane of the projection is parallel to the rake face. For simplicity, the approximate locations of the  $y$ - and  $z$ -axes are shown as coinciding with the W and N poles. Due to the orientation of the diamond their exact locations would be close to the E and S poles in this projection.

that cracks lying on cleavage planes have also been observed after repeated indentation [10]. This is very similar to the behaviour observed in this work. Thus, it seems reasonable to assume that wear takes place in two stages. During the initial stage of polishing by microcleavage, sufficient damage could be accumulated (particularly by the abrasive effect of the small diamond particles removed from the surface) to initiate microcracks on the surface. In the second stage, these cracks would propagate along the cleavage planes and generate large wear debris.

As shown in Figs 4 and 6b and in Table I, cracking occurs mainly along two of the four  $\{111\}$  cleavage planes on wear plane B. In order to investigate the reason for the apparent absence of large cracks on two of these planes, it is necessary to compare the tensile stress acting on the four cleavage planes. The stress field produced in a semi-infinite elastic body by a sliding spherical contact has been determined by Hamilton and Goodman [11]. However, this derivation is difficult to apply to the present case due to the peculiar geometry of the tool tip and to the anisotropic properties of the single crystal. Therefore, the analysis has been conducted in a less accurate, but simpler way by calculating the normal components

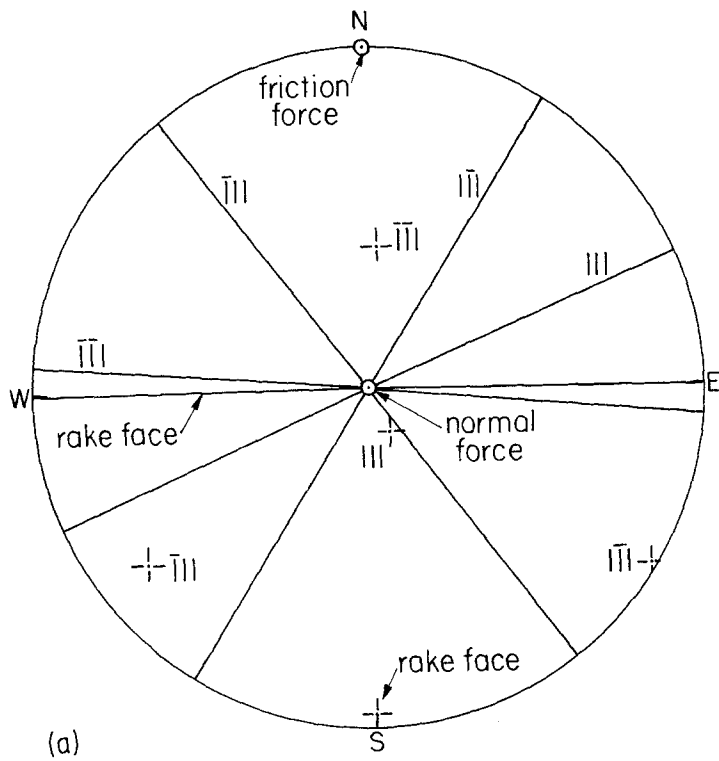
of the normal and friction forces on the four cleavage planes. If  $P$  is the force applied normal to the wear plane and  $\mu$  is the coefficient of friction, the normal component of force on a plane is

$$M = P(\pm \cos \theta_p \pm \mu \cos \theta_f) \quad (1)$$

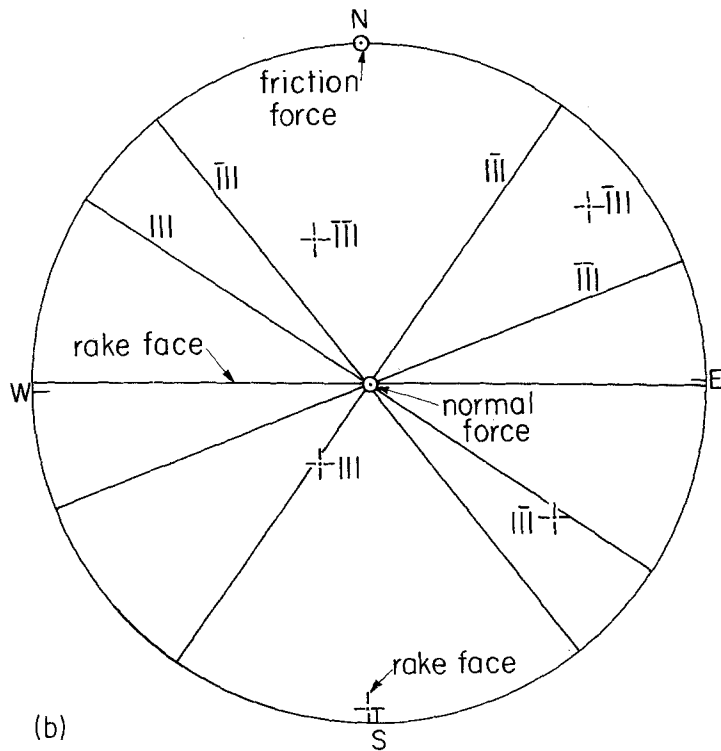
where  $\theta_p$  and  $\theta_f$  are the angles between the normal to the plane and the direction of the applied normal and friction forces, respectively. For the discussion, it is easier to consider the parameter  $n$  defined as

$$n = \frac{M}{|P|} = \pm \cos \theta_p \pm \mu \cos \theta_f \quad (2)$$

where  $M$  is normalized by the absolute value of  $P$  so that  $n$  is positive for traction and negative for compression. The discussion of the signs to apply in Equation 2 requires the examination of four different cases. These are determined on the one hand by the orientation of the plane (pole in the northern or the southern hemisphere of the stereographic projection) and on the other hand by the position of the applied force on the wear surface with respect to the trace of the plane. The applied force is defined as being in front of or behind the plane when its point of application is situated towards the clearance or towards the rake face, respectively, with respect to the trace of the plane.



(a)



(b)

Figure 6 Stereographic projections of the diamond tool used for machining tests on glass: (a) projection parallel to the wear plane A and (b) projection parallel to wear plane B.

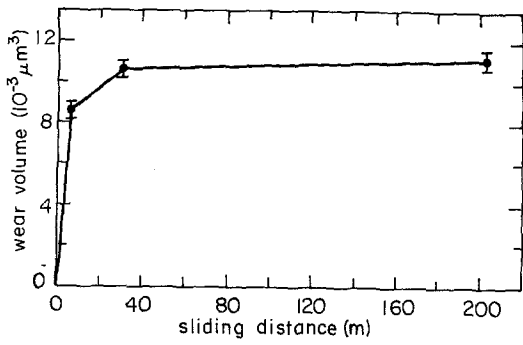


Figure 7 Wear volume as a function of sliding distance for a diamond tool rubbed against soda-lime glass.

Figure 8 Variation of the parameter  $n$  with the coefficient of friction  $\mu$  for the four cleavage planes on the wear zones of the diamond tool used for machining tests on glass. Only the highest non-zero value of  $n$  is reported for each plane.

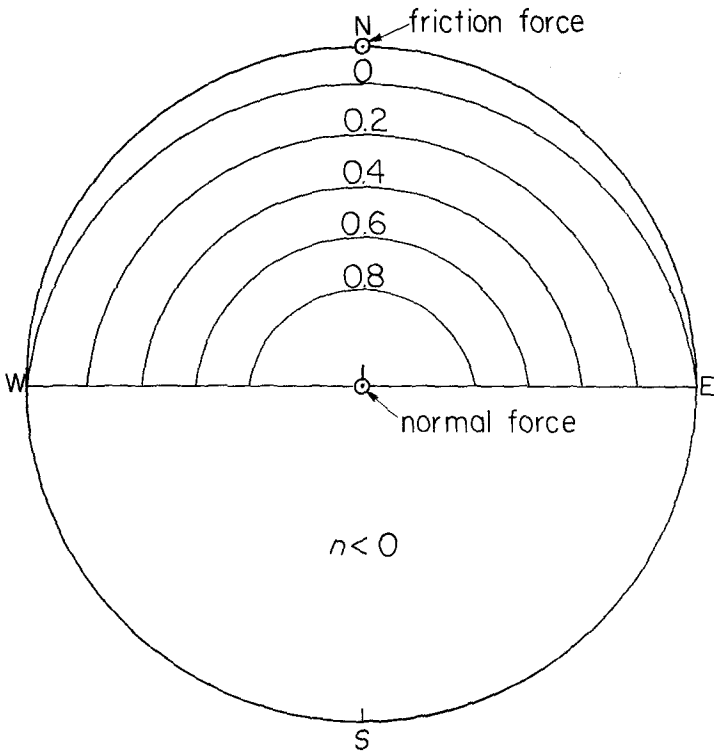
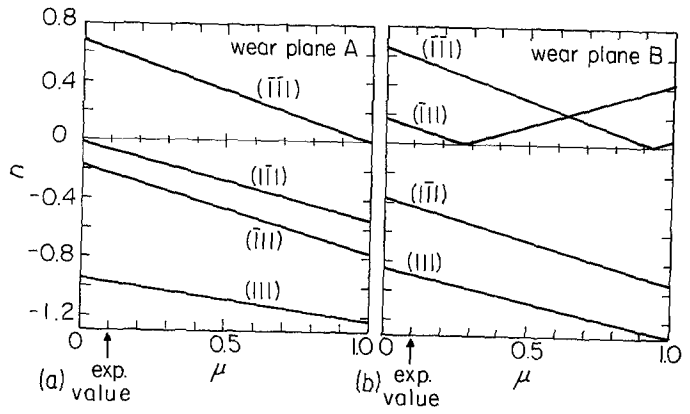


Figure 9 Dependence of the parameter  $n$  on the crystallographic orientation for a coefficient of friction  $\mu = 0.1$ . The stereographic projection is parallel to the wear plane.

TABLE II Dependence of the parameter  $n$  on the orientation of the plane and on the position of the force

Position of the force	Orientation of the plane	
	Pole in the northern hemisphere	Pole in the southern hemisphere
In front of the plane	$n = -\cos \theta_p + \mu \cos \theta_f$	$n = 0$
Behind the plane	$n = \cos \theta_p - \mu \cos \theta_f$	$n = -\cos \theta_p - \mu \cos \theta_f$

The equations relevant for the four possible cases are given in Table II. No force ( $n = 0$ ) is considered to be transmitted through the plane in case 3 because of the proximity of a free surface (rake face) on which, judged by the absence of wear, no force is exerted.

The angles  $\theta_p$  and  $\theta_f$  can easily be measured from the stereographic projections of Fig. 6. The value of  $n$  is reported as a function of the coefficient of friction in Fig. 8, according to the equations given in Table II. For the average value of the coefficient of friction ( $\mu = 0.1$ ) measured during the experiments, on wear plane A, positive values of  $n$  are possible only on one of the four cleavage planes (Fig. 8a). This might be one of the reasons why no fracture is observed in this case. On wear plane B (Fig. 8b),  $n$  is positive for the two cleavage planes  $(\bar{1}\bar{1}1)$  and  $(\bar{1}11)$  and negative for  $(1\bar{1}1)$  and  $(111)$ . This is in agreement with the observation of fracture only in the first two planes. Thus, it seems that the occurrence of cracking is mainly determined by purely geometrical considerations.

As only positive values of  $n$  are dangerous, the equations of Table II determine two main regions with respect to the orientation of the cleavage planes. If the pole is in the northern hemisphere,  $n$  is positive and tension will be exerted on the cleavage plane. On the contrary, if the pole lies in the southern hemisphere,  $n$  is negative and the cleavage plane is in compression. This strong dependence on the orientation is illustrated by Fig. 9. On this stereographic projection, similar to those of Fig. 6, lines of constant positive  $n$  have been drawn. Comparison of Figs 6b and 9 indicates immediately why preferred cracking occurred on planes  $(\bar{1}\bar{1}1)$  and  $(\bar{1}11)$  on wear plane B. It must be recalled that Fig. 9 represents an ideal case based on a rough analysis. Thus, the results must be interpreted with caution. This is especially true for the border-line cases defined by  $\theta_p \simeq 0^\circ$  and  $\theta_p \simeq 90^\circ$  for which the finite dimension of the

tool and its particular geometry should have a strong influence.

In spite of the limitations inherent in the above analysis, the agreement with the experimental results appears to be quite good. It suggests that the crystallographic orientation of the tool is extremely important as a proper choice might delay, restrict, or perhaps even eliminate the occurrence of fracture and high wear rate.

## 5. Conclusion

The investigation of a worn diamond tool used for machining tests on glass and the results of additional wear tests have led to the following conclusions. The wear process generates the formation of a wear plane, on the tool edge, which is parallel to the surface of the workpiece. This permits a simple calculation of the volume loss on the basis of purely geometrical considerations. Wear appears to proceed by two successive different processes. A polishing mechanism attributed to very fine micro-cleavage starts first. After an incubation period, the corresponding wear rate appears to remain very low. This process is eventually followed by crack propagation along cleavage planes which produces the removal of relatively large debris from the wear plane. This is believed to correspond to a high wear rate and a rapid deterioration of the tool. This mechanism appears also to be strongly dependent on the crystallographic orientation. This suggests that tool life could be improved by a careful characterization of the diamond and proper use according to the crystallographic orientation.

## Acknowledgements

The diamond tools were supplied by the Lawrence Livermore National Laboratory of the University of California. We wish to thank the Commission de Recherche, EPF, Lausanne, Switzerland and the Fonds National Suisse de la Recherche Scientifique, Berne, Switzerland for the support of this work.



## References

1. G. M. SANGER and P. C. BAKER *Soc. Photo-Opt. Instrum. Eng. Space Optics* **183** (1979) 139.
2. R. BREHM, K. VAN DUN, J. C. G. TEUNISSEN and J. HAISMA, *Precision Engineering* **1** (1979) 207.
3. J. H. GIOVANOLA and I. FINNIE, *J. Mater. Sci.* **15** (1980) 2508.
4. A. M. FRANK, J. B. BRYAN and R. W. CLOUSER, *Appl. Optics* **17** (1978) 671.
5. F. P. BOWDEN and H. G. SCOTT, *Proc. Roy. Soc. A* **248** (1958) 358.
6. J. WILKS, *Nature* **243** (1973) 15.
7. J. E. FIELD, in "The Properties of Diamond", edited by J. E. Field (Academic Press, London, 1979).
8. J. C. JAEGER, *Proc. Roy. Soc., New South Wales* **76** (1942) 203.
9. E. M. WILKS and J. WILKS, *J. Phys. D* **5** (1972) 1902.
10. J. G. BELL, M. E. C. STUIVINGA, A. G. THORNTON and J. WILKS, *ibid.* **10** (1977) 1379.
11. G. M. HAMILTON and L. E. GOODMAN, *J. Appl. Mech., Trans. ASME* **33** (1966) 371.

Received 6 October and accepted 9 December 1980.